



Flammability, smoke production, and mechanical properties of thermoplastic polyurethane composites with an intumescent flame-retardant system and nano-silica

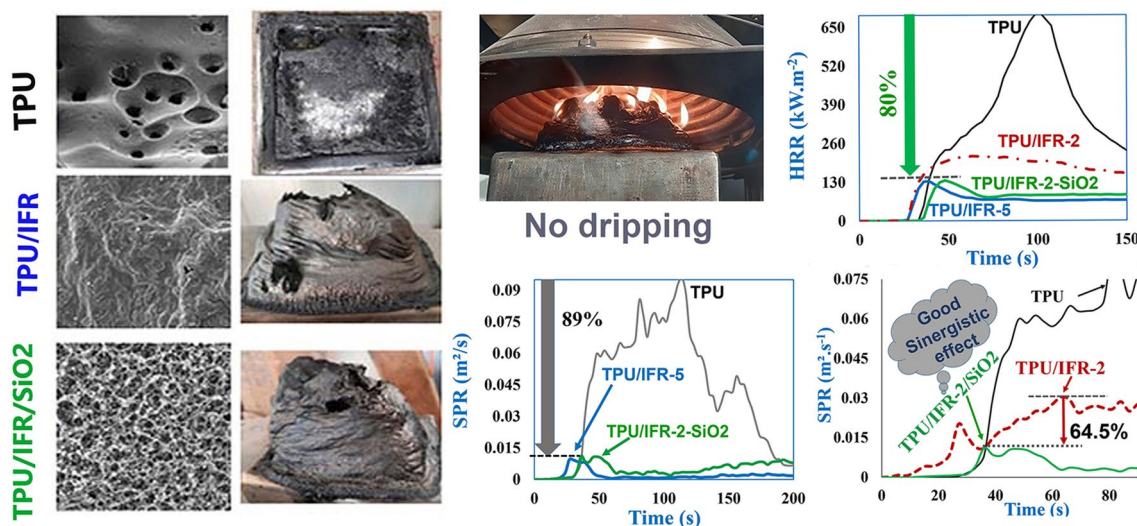
Leila Taghi-Akbari¹ · Mohammad Reza Naimi-Jamal¹ · Shervin Ahmadi²

Received: 28 January 2023 / Accepted: 14 May 2023 / Published online: 7 July 2023
© Iran Polymer and Petrochemical Institute 2023

Abstract

The aim of this work is to enhance the fire safety of thermoplastic polyurethane (TPU) composites by developing an intumescent flame-retardant (IFR) system consisting of ammonium polyphosphate (APP), melamine polyphosphate (MPP), and pentaerythritol (PER), with nano-silica as synergist. TPU/IFR composites were prepared with various APP/MPP/PER ratios and the optimal ratio of these flame retardants was determined. The cone calorimeter results showed superior fire performance of the TPU/IFR composites. The combination of 40 wt% APP, 10 wt% MPP, and 1 wt% PER significantly decreased the peak heat release (PHRR) and smoke production rates (SPR) by 80% and 89.6%, respectively, with little dripping, and without significant deterioration of mechanical properties. The char morphology with SEM technique revealed a porous char structure. The good synergistic effect of nano-silica was confirmed when the addition of 1 wt% nano-silica to the TPU/IFR with APP:PER ratio 4:1 strengthened the char structure, removed droplets, and reduced PHRR and SPR by 38% and 64.5%, while maintained the mechanical properties. All TPU composites fulfilled UL-94 V-0 grade with the limiting oxygen index (LOI) of 23–36%. TGA analysis indicated that thermal degradation of the IFR-TPUs started at a lower temperature than that of the neat TPU, indicating the earlier decomposition of IFR leading to the increase of char formation up to 25% compared with the 0.2% in the neat TPU. This work introduced a new formulation of a flame-retardant system for TPU with highly efficient flame retardant and smoke suppression properties without loss of mechanical properties.

Graphical abstract



Extended author information available on the last page of the article

Keywords Thermoplastic polyurethane · Flammability · Intumescent flame retardant · Nano-silica · Smoke suppression · Heat release

Introduction

Thermoplastic polyurethane (TPU) is one of the most important engineering plastics. TPUs are widely used in many industrial fields, such as automobiles, buildings (roof and floor coatings), films, electronics, cable sheathing, and medicine. This broad field of application is related to some excellent properties, such as chemical resistance, abrasion resistance, weather resistance, high tensile strength, high toughness, high strength, high damping, and resistance to aging [1–3].

However, the widespread use of TPU is limited due to high flammability, significant smoke emissions, and melting droplets [4]. For these reasons, improving the fire performance of TPU, especially in applications, such as aircraft, construction, electronic automobiles, and cables that are required to meet fire safety requirements, is necessary. From the viewpoint of fire safety, reducing heat release and smoke production, as far as possible, preventing melt dripping during the burning of polymers, are critical. Hence, different flame retardants (FRs), including reactive and additive, have been developed for this purpose [5–7].

Nowadays, halogen-containing flame retardants (HFRs) are substituted by various halogen-free flame retardants because of environmental aspects such as low smoke and low toxicity [8, 9]. Among the wide range of flame-retardant additives (FRs), intumescent flame retardants (IFRs), as environmentally friendly flame retardants, have high flame-retardant efficiency, and a lot of research works has been done on this issue [10–12]. Generally, the IFR systems have three primary constituents as followings: (a) an acid source such as ammonium polyphosphate (APP), (b) a blowing agent or gas source such as melamine, and (c) a charring agent such as pentaerythritol (PER) [13].

It has been found that APP cannot form an effective intumescent system alone [14], and a combination of FR additives may be needed to achieve reasonable flame retardancy. One of the effective strategies is the use of synergistic agents, such as carbon fibers, nano-fillers (such as SiO_2 and MoS_2) with the IFR systems as a flame retardant, and smoke suppressant [4, 15, 16]. The advantages of these flame retardants are low loading and improvement of mechanical, thermal, and electrical properties [17]. Chen et al. [18, 19] showed that the synergistic agent even changes the char residue structure of the TPU/APP composites. Martin et al. provided a detailed discussion about the TPU nanocomposites and the effects of nano-fillers

on the TPU morphology and mechanical and biological properties [20].

One of the effective nano-fillers is nano-silica which has obtained much attention due to improvement in the thermal, rheological, and mechanical properties of TPU [21, 22]. A reason for this improvement is the creation of hydrogen bonds between the nano-silica particles and the soft segments of TPU polymer contributing to the phase separation [23]. Nano-silica with a high surface area and tiny particle size, used as reinforcement in elastomers particularly, restricts the oxygen penetration into the polymer during combustion and reduces heat and smoke production and flame spread, consequently. This is highly significant, especially when flame retardancy aims to give more time to escape occupants of buildings in case of fire.

According to previous studies [24, 25], high loading of conventional flame retardants (more than 20 wt%) can result in poor smoke suppression and relatively lower flame-retardant efficiency. Moreover, it was reported that a high loading level of APP in flame-retardant TPU/APP composites was needed to achieve satisfactory flame retardancy, which led to the deterioration of mechanical properties [25, 26]. However, as the results of the tests showed, the new formulation of an IFR system developed in the present research work did not deteriorate the mechanical properties of the produced TPU composite, in spite of applying relatively high content.

In the present work, IFR systems consisting of ammonium polyphosphate (APP), melamine polyphosphate (MPP), and pentaerythritol (PER) with different weight ratios were added to a polyester-based TPU by melt blending method. Keeping the APP content constant, different loadings of MPP/PER were applied. The optimal MPP:PER ratio was determined using flammability tests, including LOI, UL-94 vertical burning test, and cone calorimeter test (CCT). Then, the influences of nano-silica (N-Si) were investigated on the heat and smoke suppression, anti-dripping, and char structure of a selected TPU/IFR composite generating more smoke than the other prepared composite samples. The effect of the amounts of the IFR constituents on the fire safety of TPU/IFR composites was also studied.

Three aspects of fire safety, including heat release, smoke production, and melt dripping, were comprehensively discussed. Two methodologies were used to evaluate the fire hazard of the TPU/IFR composites based on thermal parameters obtained from the cone calorimeter test results: calculation of fire performance index (FPI) [6] and the proposed classification by Bakhtiyari et al. [27]. The best formulations

of IFR-TPU composites were selected to further study their thermal stability (TGA), microstructure (FTIR), char morphology (SEM), and mechanical properties.

This research work aimed to develop a new formulation of an intumescent flame-retardant (IFR) system consisting of APP/PER/MPP with the possibility for high loadings of its constituents in TPU to achieve highly efficient flame-retardant properties without deterioration of its mechanical performance. To the best of our knowledge, no similar research has been reported on this area.

Experimental

Materials

A polyester-based thermoplastic polyurethane (TPU), (Estane[®] 58277) produced by Lubrizol (USA) was used as a polymer matrix. APP (Exolit[®] AP 422) was obtained from Clariant (Switzerland). Melamine polyphosphate (Melapur200) was obtained from BASF (Germany), and pentaerythritol (PER) was supplied by the MERCK (Germany). Nano-silica was supplied by Wacker Chemie (Germany) with an average particle size of 50 nm and a specific surface area of 175–225 m²/g.

Sample preparation

Before melt blending, TPU was dried in an oven at 80 °C for 12 h. The IFR components, including APP, MPP, and PER, were dried in a vacuum oven at 100 °C for 10 h. Then, the IFR components were mixed. A certain amount of TPU was melted in a Bra bender mixer, and the IFR system was added into the mixer at 170 °C, with a rotation speed of 40 rpm, for 6 min. Nano-silica (N-Si) was mixed with the TPU/IFR at a rotation speed of 70 rpm, and it took about 5 min to make a homogenous nanocomposite. All blends were pressed into sheets using a press machine at 130 °C under 10 MPa for 10 min. The thicknesses of the samples were about 3 mm. The formulations of the flame-retardant TPU composites are listed in Table 1.

As shown in Table 1, three formulation types were applied to prepare TPU/IFR composites: in the first type, keeping the amount of APP constant at 40.0 wt%, PER, or MPP was used with 10 wt% (TPU-1 and TPU-2) in which the weight ratio of APP/MPP or APP/PER was 4/1. In the second type, equal amounts of MPP/PER by 10 wt% were used (TPU-3). In the last type, MPP/PER weight ratios of 1/10 and 10/1 were used (TPU-4 and TPU-5).

To investigate the synergistic effect, 1 wt% of nano-silica was separately added to two TPU/IFR composites (TPU-2 and TPU-1 formulations) and two nanocomposites (TPU-6 and TPU-7) were prepared.

Characterization

The limiting oxygen index (LOI) was measured according to ASTM D2863 using the HC-2 oxygen index meter (Karangin Co.) The dimensions of the specimens used were (130 × 6.5 × 3.2) mm³.

The UL 94 vertical burning test was performed according to the ASTM D3801 test method. The dimensions of the test specimens were 130 × 13 × 3.2 mm³.

Thermogravimetric analyses (TGA) were carried out at 20 °C/min under a nitrogen atmosphere using a TGA-Mettler (Mettler Toledo, Switzerland) instrument. Each sample was heated from ambient temperature to 600 °C. Then, the sample was heated to 800 °C in air flow at 20 °C min⁻¹.

FTIR spectra were recorded with a Bruker Equinox55 (USA) FTIR spectrometer in 400–4000 cm⁻¹. The solid product was mixed with KBr powder, and the tested samples were obtained by a pelletizer.

The flammability was measured by an FTT dual-cone calorimeter apparatus (Fire Testing Technology, UK). The bench-scale fire tests were performed according to ISO 5660-1 standard test method under a radiant heat flux of 50 kW m⁻². The dimensions of the TPU/IFR samples were (100 × 100 × 3) mm³. Each specimen was wrapped in aluminum foil and exposed horizontally to the heat flux.

Scanning electron microscopy (SEM) was performed using a VEGA\TESCAN-LMU (Czech Republic)

Table 1 Formulations of TPU/IFR composites

| Sample code | TPU (wt%) | APP (wt%) | MPP (wt%) | PER (wt%) | N-Si (wt%) | UL-94 rating |
|-------------|-----------|-----------|-----------|-----------|------------|--------------|
| TPU-0 | 100 | 0 | 0 | 0 | 0 | No rating |
| TPU-1 | 50 | 40 | 10 | 0 | 0 | V0 |
| TPU-2 | 50 | 40 | 0 | 10 | 0 | V0 |
| TPU-3 | 50 | 30 | 10 | 10 | 0 | V0 |
| TPU-4 | 49 | 40 | 1 | 10 | 0 | V0 |
| TPU-5 | 49 | 40 | 10 | 1 | 0 | V0 |
| TPU-6 | 49 | 40 | 0 | 10 | 1 | V0 |
| TPU-7 | 49 | 40 | 10 | 0 | 1 | V0 |

scanning electron microscope at 15 kV acceleration voltage. Gold coating of the samples was performed before scanning.

The mechanical properties of TPU/IFR composites were characterized at room temperature according to ASTM D638 by a universal test machine (APS Co., Iran).

Shore-A hardness was also measured by a digital shore hardness tester according to ASTM D2240.

Results and discussion

Flammability

Flammability of TPUs, including the neat TPU (TPU-0) and flame retarded TPU composites, was characterized by LOI. LOI indicates the minimum oxygen concentration (volume percentage) required to burn the specimen. Material having an LOI of less than 21% can burn easily, but if LOI be greater than 21%, flammability decreased after removing the ignition source [28].

Figure 1 shows the LOI values for the TPU/IFR samples. The UL-94 results are given in Table 1. TPU-0 ignited and melted fast with high dripping, and no rating was obtained. The incorporation of the IFR system in the TPU increased LOI values to 34% with reduced melt dripping. The LOI value reached 36% in the TPU-6 which was due to the effective synergy between nano-silica and IFR leading to high-efficiency flame retardancy; while the LOI value reached 28% in the TPU-7. An important reason for this difference is the effect of the charring agent (PER) which was absent in the TPU-7 formulation. In other words, with the presence of a protective intumescent char layer at the surface of the TPU-6, a higher oxygen content was required to sustain the combustion of the specimen. As a result, the LOI value for TPU-6 was more than that of TPU-7. UL-94 V-0 rating was achieved for all flame-retardant TPU/IFR composites.

Flame retardancy, smoke suppression, and fire hazard

Cone calorimeter tests were performed on the prepared composites to assess the fire hazard. A cone calorimeter is one of the best research apparatuses for studying the fire behavior of materials on a small scale. This apparatus can evaluate ignitability, heat and smoke production (rate and total), and CO/CO₂ toxicity. Its results are valuable for the simulation of real fires. Babrauskas and Peacock [29] showed that heat release rate (HRR) is the single and most crucial variable for evaluating the fire hazard of materials. Some key thermal and smoke parameters obtained from the cone calorimeter tests are listed in Table 2. Figures 2, 3, 4 show heat, smoke release, and residual char curves, respectively.

Thermal parameters

Heat release rate (HRR) is the most critical parameter to assess the fire hazard of polymers. The HRR curves of all TPU specimens are shown in Fig. 2. Based on the HRR curves, TPU-0 showed the highest PHRR value of 696.3 kW m⁻² at 102 s. It burned easily after ignition with high melt dripping. By incorporating IFR with an APP/MPP ratio of 4/1 into TPU-1, the PHRR value decreased sharply to 323 kW m⁻², which was about half of the PHRR value of TPU-0. At the same time, the char residue percentage reached 21% compared with 7.5% in the origin TPU.

According to the previous studies [30–32], APP accelerated the TPU decomposition leading to the formation of a phospho-carbonaceous polyaromatic structure acting like a protective layer during burning. Besides, thermolysis of MPP can produce ammonia gas and reduce accessibility to oxygen and enhance the char at the surface of TPU. Therefore, flame retardancy was achieved. Interestingly, the peak heat release of TPU-2 with APP/PER: 4/1 showed a further decrease and reached 216 kW m⁻² and the char residue of 22%. In addition, the ignition time was shorter. These results were in agreement with the findings of Li et al. [32]. They found that PER carbonized under the effect of the strong acid

Fig. 1 Variation of LOI values for TPU/IFR composites

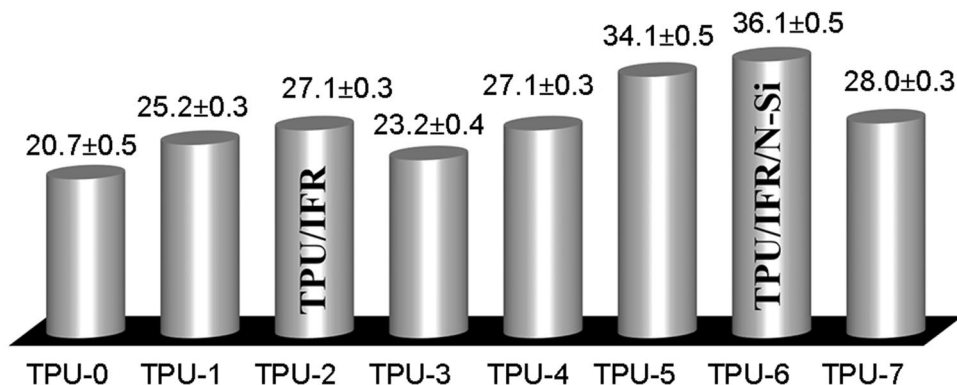


Table 2 Cone calorimeter data for TPU/IFR composites/nanocomposites

| Sample code | Thermal parameters | | | | Smoke parameters | | | Residual mass (%) | Fire hazard FPI (m ² s kW ⁻¹) |
|-------------|--------------------|----------------------------|------------------------------|---------------------------|---|---|--------------------------|-------------------|--|
| | TTI (s) | PHRR (kW m ⁻²) | HRRave (kW m ⁻²) | THR (MJ m ⁻²) | Av.SEA (m ² kg ⁻¹) | pSPR (m ⁻² s ⁻¹) | SF (MW m ⁻²) | | |
| TPU-0 | 37 | 696.30 | 178.63 | 51.40 | 257.36 | 0.096 | 670.40 | 7.5 | 0.05 |
| TPU-1 | 36 | 323.07 | 148.14 | 75.47 | 283.82 | 0.051 | 278.07 | 21.2 | 0.11 |
| TPU-2 | 33 | 216.19 | 117.65 | 71.38 | 419.49 | 0.031 | 252.40 | 22.1 | 0.15 |
| TPU-3 | 27 | 273.76 | 109.79 | 78.04 | 237.58 | 0.030 | 204.77 | 16.6 | 0.10 |
| TPU-4 | 33 | 278.30 | 157.95 | 73.64 | 308.30 | 0.042 | 247.63 | 21.5 | 0.12 |
| TPU-5 | 33 | 132.54 | 48.23 | 29.77 | 98.11 | 0.010 | 36.20 | 40.6 | 0.25 |
| TPU-6 | 43 | 135.00 | 47.65 | 31.65 | 147.19 | 0.011 | 53.06 | 44.2 | 0.32 |
| TPU-7 | 35 | 360.51 | 165.24 | 60.56 | 339.83 | 0.051 | 273.05 | 22.5 | 0.10 |

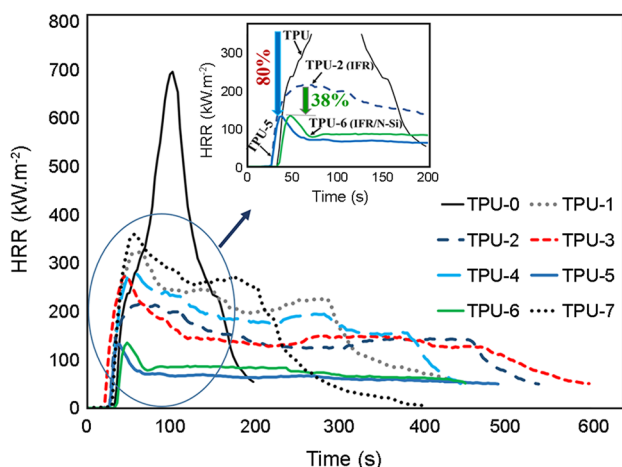


Fig. 2 HRR curves of TPU/IFR composites at flux of 50 kW m⁻²

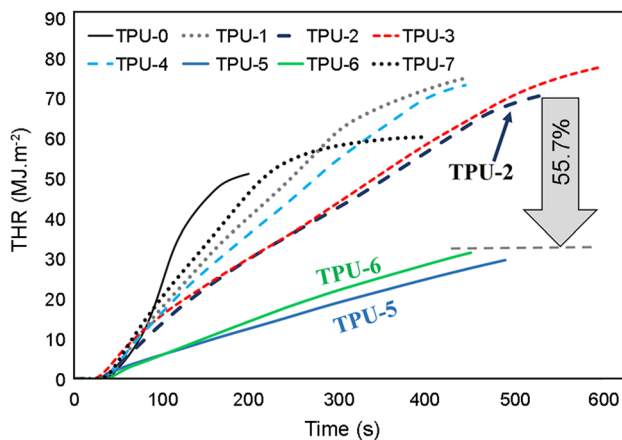


Fig. 3 THR curves of TPU/IFR composites at flux of 50 kW m⁻²

APP at a specific temperature, and the char layer formed. Through incorporation of IFR contents by MPP/PER ratios of 1/10 (TPU-4) and 10/1 (TPU-5) with APP at constant

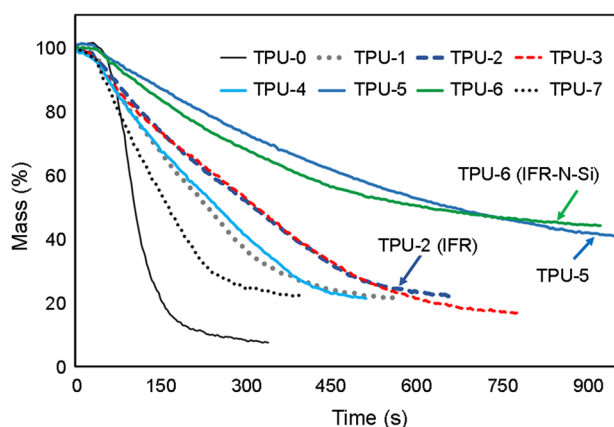


Fig. 4 Mass loss curves of TPU/IFR composites at flux of 50 kW m⁻²

amount of 40 wt%, PHRR reduced dramatically compared with the TPU-0, especially in the TPU-5, which showed the lowest PHRR by 132.5 kW m⁻². In other words, it was 80.9% less than the reference TPU (TPU-0).

In the third formulation (TPU-3), with an MPP/PER ratio of 1/1 and reducing the APP loading to 30 wt%, the time to ignition was lower than the other TPU composites and PHRR reached 273.8 kW m⁻² while char residue was lower than the other TPU composites.

Such systematic set of flame retarded TPU samples with different concentrations of flame retardants, including melamine polyphosphate (MPP), melamine cyanurate (MC), and aluminum diethylphosphinate (AlPi) with a total amount of additives 30 wt%, were investigated by Sut et al. [5]. The findings showed that with a constant AlPi load, the best fire behavior was obtained by the 10/15/5 ratio (MPP/MC/AlPi) with a PHRR reduction of 77% and V-0 classification in the UL 94 test. There were no data for smoke parameters.

The residual mass after burning TPU-5 was twice that of TPU-1, TPU-2, and TPU-4 by 40.6% compared with 22%. In this case, it can be said that the phosphorus–phosphorus

synergism of APP with melamine salt of pentaerythritol acid phosphate, as stated by Weil [33], was stronger in TPU-5. The synergistic effect of nano-silica on the thermal parameters of TPU and TPU/IFR was also notable. By introducing nano-silica by 1wt% into TPU-2 composite sample, the highest char residue of 44.2% was formed in the TPU-6 nanocomposite which was almost six times that of TPU-0. PHRR was also reduced by 37.6% compared with TPU-2 and 80% compared with TPU-0 (Fig. 2). A remarkable point of TPU-7 nanocomposite was the effect of the carbon source (PER), which compared to TPU-6, the amount of residual mass was half of that of TPU-6. In addition, due to the role of char formed as a thermal barrier, the amount of PHRR was higher than that of TPU-6.

Effects of the weight ratio of APP/PER on the flame retardancy, properties of phosphorous degradation products, and char structure were investigated by Xia et al. [34] for polypropylene/IFR (APP/PER). They reported that the APP:PER ratio had a great effect on the flame-retardant properties and char structure which in turn affected mass and heat transfer. Our study confirms this, especially for TPU-6 and TPU-7, these effects were evident.

Bourbigot et al. [35] expressed a considerable reduction in PHRR could be achieved using silicon-containing additives alone, e.g., polyhedral oligomeric silsesquioxane (POSS) in TPU. The current work showed a significant reduction in PHRR by a low amount of nano-silica as a flame-retardant synergist with IFR, as observed in TPU-5 and TPU-6 with considerable suppression of heat release as well as the highest residual mass.

The curves of total heat release (THR) of all TPU samples in Fig. 3 indicate that THR value of TPU-0 (51.4 MJ m⁻²) was higher than those of the TPU-5 and TPU-6, but the other samples showed a higher THR than the origin TPU. The gradient of the THR curve represents flame spread [36, 37]. Therefore, the lower slope of THR curves in the flame-retardant TPU composites indicates a slow-flame spread. Figure 3 also shows that the synergistic flame-retardant property between nano-silica and TPU-2 plays an important role in the THR reduction (55.7% decrease).

The mass loss curves of all TPU samples are presented in Fig. 4. Mass loss is a crucial parameter in the interpretation of flame retardancy and smoke suppression. It can be seen in Table 2 and Fig. 4 that the mass of the TPU-0 showed a sharp decline in the range of 20–200 s, and only 7.5% mass remained at the end of the test.

In the case of the TPU composites, the mass residue was higher than that of TPU-0. In TPU-1, TPU-2, TPU-4, and TPU-7 samples, the remained char residue after the cone calorimeter test was nearly three times that of the pure TPU (about 22%). This could be attributed to the formation of a protective char layer in the TPU/IFR composites reducing heat transfer to the underlying composite and accessibility to oxygen. Therefore, the release of heat and volatile compounds was reduced. In other words, the composition of IFR (i.e., APP, PER, and MPP) affected the flame retardancy of the TPU/IFR composites, substantially. The mass loss of TPU-5 sample with a char residue mass of 40.6% was the lowest among all TPU/IFR composite samples.

However, the mass loss of TPU-6 with a char residue of 44.6% was even lower than that of TPU-5. According to previous studies [38], it was attributed to the nano-silica effect which could increase the melt viscosity in the intumescent systems and promote the highly expanded char formation, limiting the heat and pyrolysis gases with low mass loss and strengthened mechanical properties. Besides, migration of the nano-silica particles onto the surface of the TPU nanocomposite during burning was the second factor in increasing the char yield. The char formed in the TPU-6 nanocomposite sample was compact and its residual yield was more than that of the other TPU/IFR samples. These phenomena were in agreement with the TGA and SEM results.

The cooperation between IFR and nano-silica strengthened the char residue and removed dripping. The digital photographs of the char residues obtained from the TPU and flame-retardant TPU composites are shown in Fig. 5.



Fig. 5 Photos of char residue of TPU/IFR composites after cone calorimeter test

Smoke parameters

Most fire deaths are due to smoke and toxic gases that influence the respiratory system, reduce visibility, and critically affect rescue and evacuation. Hence, smoke suppression with various flame retardants is always a significant issue. As mentioned earlier, TPU is flammable and generates lots of melt droplets, toxic gases, and smoke during combustion, posing a severe threat to people's lives in fire events [39]. Thus, the smoke release is one of the critical factors in evaluating the fire safety of materials in real fires.

Smoke production rate

As a key smoke parameter, smoke production rate (SPR) is obtained from cone calorimeter test and determines the amount of smoke produced by a surface area of one square meter of material per second during combustion. As depicted in Fig. 6, the SPR of IFR-TPU composites were specifically reduced by addition of IFR and nano-silica, especially in TPU-5 and TPU-6 samples. It can be seen that the peak of SPR (pSPR) for TPU-1 was reduced by about 50% compared to the neat TPU and reached $0.051 \text{ m}^2 \text{ s}^{-1}$ compared to 0.096 at 114 s for TPU-0 sample. In the case of TPU-5, the pSPR showed the lowest value of $0.01 \text{ m}^2/\text{s}$ at 27 s and exhibited reduced smoke production by 89.6%. What is more, the time to pSPR (27 s) was dramatically lower than that of TPU-0 (114 s) which represents the earlier decomposition of IFR at a lower temperature to form carbon layer and smoke particulates. The protective char layer on the composite surface reduces smoke-forming materials in the gas phase leading to a decrease in SPR [40].

The same result was observed for TPU-6 in which nano-silica by 1.0 wt% had been added to TPU-2 sample. The

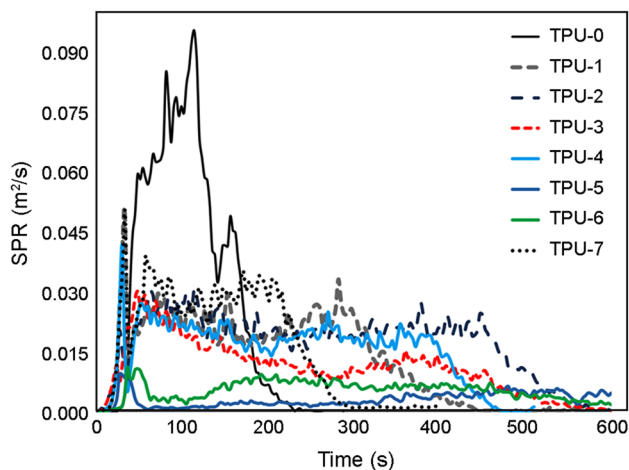


Fig. 6 Variation of smoke production rate (SPR) for TPU/IFR samples at flux of 50 kW m^{-2}

pSPR value of TPU-6 was $0.011 \text{ m}^2 \text{ s}^{-1}$ at 36 s, which was decreased by nearly 65% compared to TPU-2 and 88.5% compared to the origin TPU, as shown in Fig. 7. It is confirmed that nano-silica is an effective smoke suppression and flame-retardant synergist in TPU/IFR composites. A meaningful topic here is the influence of the PER as a carbon source which enhanced the thermal barrier with increasing quality of char during the combustion of the TPU/IFR composite. As seen in the heat and smoke suppression for TPU-6 in comparison with TPU-7 in spite of the nano-silica as a synergist.

Average specific extinction area

Specific extinction area (SEA) is a measure of smoke obscuration potential per unit mass burnt. It is assumed that obscuring particles are opaque spheres blocking the light path. Average SEA (Av.SEA) is a critical smoke parameter which shows the smoke obscuration. It is so important, because blurring of vision due to smoke emission is an effective factor in the escape of people in a fire and research works have also been completed in this field [41].

According to the data in Table 2, changes did not have a regular trend, but in the two samples of TPU/IFR composites, i.e., TPU-5 and TPU-6, their values were significantly reduced compared to TPU-0. It also figured out that nano-silica had a significant effect on reducing Av.SEA for TPU-2 by a value of $419.47 \text{ m}^2 \text{ kg}^{-1}$ and for TPU-6 by a value of $147.19 \text{ m}^2 \text{ kg}^{-1}$, as presented in Table 2.

Smoke factor

Figure 8 gives the smoke factor (SF) for all TPU/IFR composite samples. SF is the product of PHRR and TSR [42].

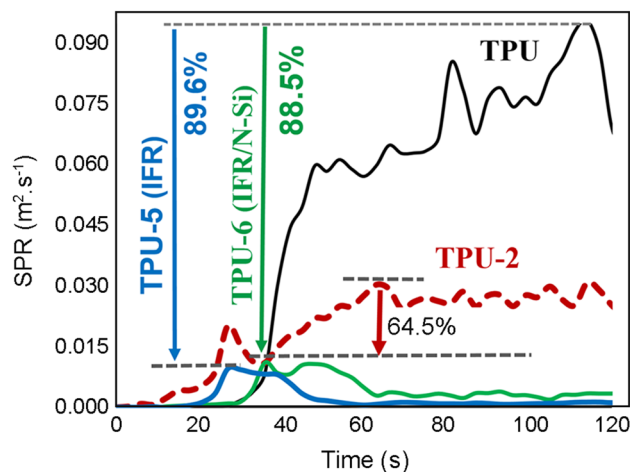


Fig. 7 Plots of smoke suppression in TPU/IFR composites (TPU-5 and TPU-6) and synergistic effect of nano-silica

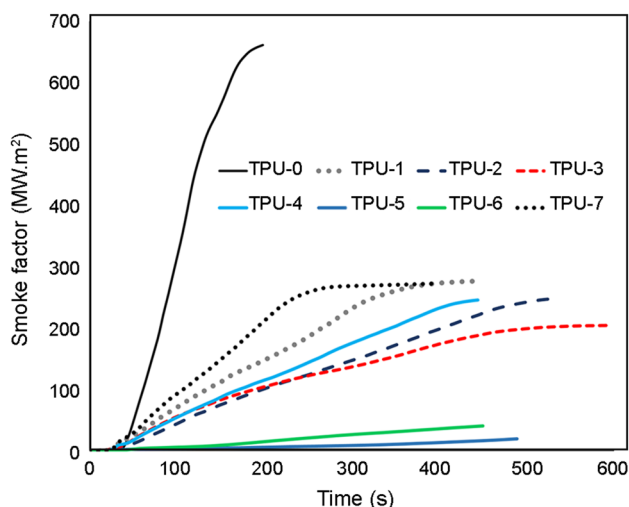


Fig. 8 Plots of smoke factor (SF) for TPU/IFR samples at flux of 50 kW m^{-2}

The SF value of TPU-0 was up to 670.4 MW m^{-2} , and the SF value of TPU-1 containing APP and MPP specifically was reduced to 278.1 MW m^{-2} . This decreasing trend was valid in all TPU/IFR composite samples. It is clear that the addition of the IFR system and nano-silica significantly reduced the SF values of TPU/IFR composites.

Moreover, the TPU-5 and TPU-6 samples showed a further decrease in SF values compared with the other flame-retardant TPU samples, where the SF values of TPU-5 and TPU-6 samples were 36.2 MW m^{-2} and 53.1 MW m^{-2} , respectively. Such phenomenon can be described as follows: during combustion, decomposition of the IFR (APP + PER + MPP) promotes the carbonization of TPU forming an intumescent protective char as a physical and thermal barrier. This char limits the heat and oxygen transfer into the polymer. Similar to such behavior has been reported by Liu et al. [43] by incorporating APP with carbon black (CB) as a smoke suppression synergist into TPU. They observed low total smoke release (TSR) and SF values in the TPU/APP/CB composites. They concluded catalyzing carbonization by APP and the synergistic effect of CB via improving the molten viscosity of carbon precursor, which enhance the char residue which effectively reduces the smoke release [43].

Fire hazard

The fire performance index (FPI) reflects fire safety. The FPI ($\text{m}^2 \text{ s kW}^{-1}$), defined as the ratio of TTI and PHRR, is a deduced parameter obtained from cone calorimeter test data for fire hazard ranking of materials [6]. A higher FPI value means a lower fire hazard, and vice versa. In another word, the materials having high FPI exhibit a lower propensity of

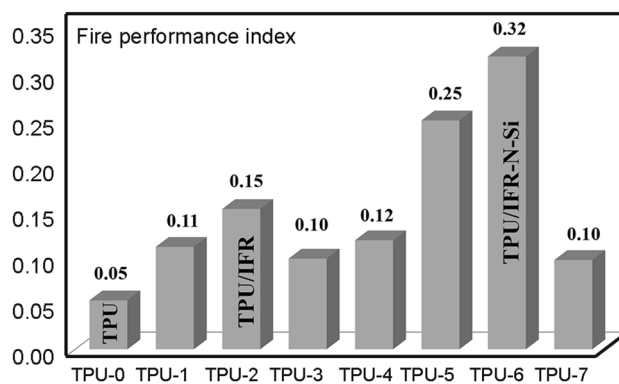


Fig. 9 Variation of fire performance index (FPI) for TPU/IFR samples

fire propagation, subsequently a longer time to flashover. This subject is critical in life safety in fire conditions.

Figure 9 shows the FPI values of TPUs based on the cone calorimeter data at a heat flux of 50 kW m^{-2} . It can be seen in Table 2 that the best fire performance was attributed to TPU-6 nanocomposite (0.32). In addition, the FPI value in TPU-5 (0.25) was also high compared with the other TPU/IFR composites. It revealed that the applied flame retardants in TPU-5 and TPU-6 samples imparted a higher safety rank than the other samples. In most of the IFR-TPU samples, TTI values were lower than that of the TPU-0 due to accelerating thermal degradation by the flame-retardant effect, but because of the reduced PHRR values significantly, the FPI values were increased.

Based on the proposed classification by Bakhtiyari et al. [27], TPU-5 and TPU-6 composite samples met the criteria of fire hazard class 2 which means a THR of 50 MJ m^{-2} or less and a PHRR of 150 kW m^{-2} or less under radiant heat flux exposure of 50 kW m^{-2} for 15 min, while the original TPU met fire hazard class 4 which is related to materials that their PHRR value was greater than 250 kW m^{-2} in the same test condition.

Thermal stability of TPU/IFR composites

Considering the cone calorimeter test data, thermal degradation, and char residues' morphology of TPU-0 and two flame-retardant TPU composites that showed the best fire performance among the samples tested, they were evaluated by TGA/DTG analyses (Figs. 10 and 11) and SEM (Fig. 12). The thermal degradation data are given in Table 3.

According to the curves, the TPU-0 started to decompose at $311.7 \text{ }^\circ\text{C}$ (T_{initial} indicating the temperature at which 5% mass loss occurs). Thermal degradation process for TPU is consisted of two main stages. The first step corresponds to the depolycondensation or the breakage of the TPU main chains and the elimination of volatile compounds. The

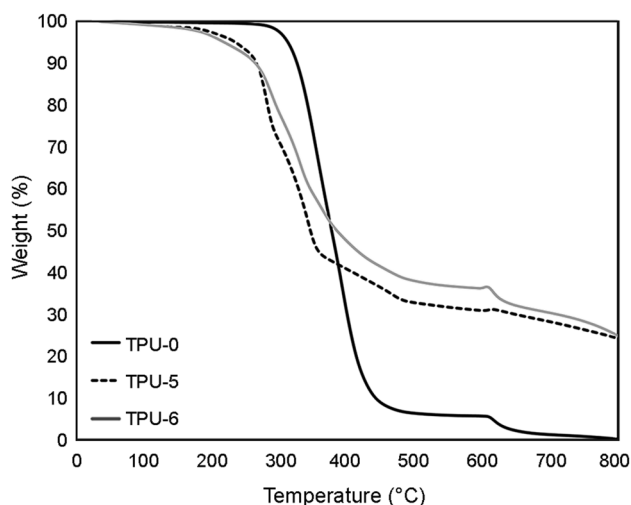


Fig. 10 TGA curves of TPU/IFR samples in N_2 /air atmosphere

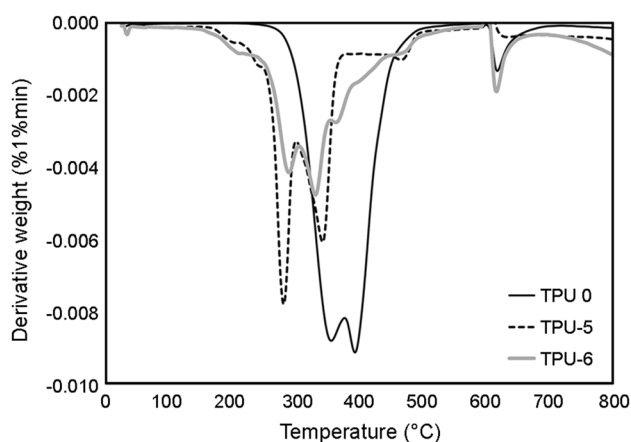


Fig. 11 DTG curves of TPU/IFR samples in N_2 /air atmosphere

second stage is related to the maximum weight loss temperature of TPU appearing at 399.7 °C, attributed to further degradation of C–C and C–O bonds [16, 44].

In the presence of the IFR system, the beginning of the first step of degradation of TPU shifted at a lower temperature than TPU-0 which is assigned to the catalytic degradation effect of the IFR system in TPU/IFR composite. As can be seen in Figs. 10 and 11, the $T_{initial}$ of TPU-5 was 233.0 °C, and three thermal degradation peaks appeared at 282.3 °C, 345.0 °C, and 474.3 °C. The first peak corresponds to the dehydration and deamination process of IFR, and the other two peaks are attributed to charring by cross-linking and more degradation and char formation, as expressed by Liu et al. [16]. The char residue at 800 °C was approximately 25% indicating the flame-retardant efficiency.

Thus, the presence of IFR system in TPU-5 affected its thermal decomposition by decreasing the thermal stability

in earlier degradation step and leading to char residue and better thermal stability at higher temperatures. It can be seen in Fig. 10 that thermal degradation of the TPU-6 nanocomposite sample had three steps, too. The $T_{initial}$ of TPU-6 was 217.0 °C, but its first T_{max} was higher than that of TPU-5 (294.3 °C) which can be related to the nano-silica effect on the TPU/IFR composite.

Consequently, the addition of APP, MPP, and PER reduced the temperature of the formation of the carbon layer, preventing further thermal degradation of TPU/IFR composites [18]. The lower decomposition temperatures of the IFR system can promote the decomposition of TPU at a lower temperature than TPU-0. Finally, the residual masses were 24.3% and 24.9% for TPU-5 and TPU-6 samples at 800 °C, respectively; while the char residue for TPU-0 was only 0.2%. The TGA results were in agreement with the mass loss results from the cone calorimeter test (Fig. 4).

Morphology and structure of char residues

The morphology of char residues of TPU-0, TPU-5, and TPU-6 samples after the cone calorimeter test was investigated by scanning electron microscopy (SEM) technique. Figure 12a–c presents SEM micrographs of the fractured surface of chars of TPU-0, TPU-5, and TPU-6 samples magnified 500×. Figure 12d presents the SEM micrograph of intumescent silica-rich char of TPU-6 sample magnified 2000×.

As shown in Fig. 12a, TPU-0 had a char with a smooth and loose surface with many holes. The pore structure contributes to gas diffusion and heat transfer, which makes the neat TPU burns readily and releases heat and smoke significantly, as seen in Table 2 for PHRR and pSPR values. Figure 12a indicates that TPU-0 formed a little char.

The charred structure of TPU-5 shown in Fig. 12b was integrated, but there were some small holes on the surface and the char formed was not dense. Figure 12c reveals that the surface of char is silica-rich. The presence of nano-silica particles on the surface of char of the TPU-6 sample formed a network-structure (Fig. 12d) acting as an excellent thermal barrier [21]. This protective carbon layer can prevent the heat transfer between the flame zone and burning polymer, and further pyrolysis of the underlying material, too.

The char residue of TPU-6 containing nano-silica with APP/PER was more condensed than that of the TPU-5 without nano-silica. This structure can strengthen the char and retard the creation and propagation of cracks. As a consequence, dripping is stopped, and flame retardancy is improved more. Besides, the emissions of heat, smoke, and CO are restricted.

According to Morgan's study [45], a condensed-phase mechanism occurs in the polymers having oxygen and nitrogen heteroatoms with phosphorus flame retardants which

Fig. 12 SEM micrographs of char residue for: **a** TPU-0, **b** TPU-5, and **c, d** TPU-6 after cone calorimeter test

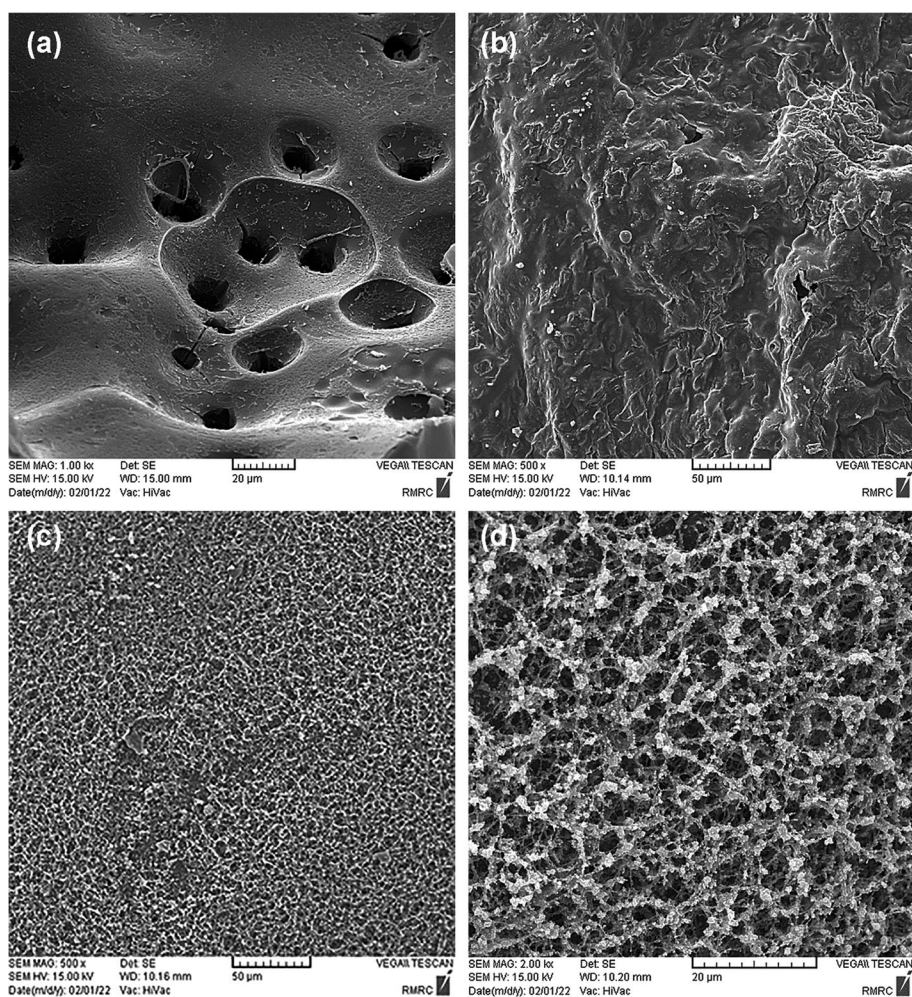


Table 3 Thermal analysis data for TPU/IFR samples

| Sample code | T_{Initial} (°C) | T_{maximum} in N_2 (°C) | | | Char residue (wt %) | |
|-------------|---------------------------|------------------------------------|--------------------|--------------------|---------------------|-----------|
| | | $T_{\text{max 1}}$ | $T_{\text{max 2}}$ | $T_{\text{max 3}}$ | At 600 °C | At 800 °C |
| TPU-0 | 311.7 | 353.0 | 399.7 | – | 5.6 | 0.2 |
| TPU-5 | 233.0 | 282.3 | 345.0 | 474.3 | 30.9 | 24.3 |
| TPU-6 | 217.0 | 294.3 | 333.0 | 477.0 | 36.2 | 24.9 |

leads to the highly cross-linked structure formation, reducing heat release and decelerating mass loss in combustion. Lim et al. [46] reviewed the application of APP in thermoplastic composites and explained how the APP worked in the dense phase as an intumescent flame retardant.

Bourbigot and co-workers [35] have studied the mechanism of intumescent char formation by an IFR system, including ammonium polyphosphate/pentaerythritol, and concluded that the main part of char composition was the linked polyaromatic species by phosphor-hydro carbonaceous bridges.

Levchik and Weil [47], in the review of the thermal decomposition, combustion, and fire-retardancy of PURs,

presented the possible thermal degradation reactions of IFR-TPUs. Based on these studies and the obtained results and TGA-DTG, FTIR, and SEM characteristics, we assume that APP reacts first with the PER and TPU matrix subsequently.

The role of the App is to promote dehydration in the initial stages of burning and char-forming. The intumescent char formation occurs by developing an aromatic phospho-carbonaceous structure with P–O–C bridges. At higher temperatures, P–O–C bridges are broken, and the final degradation occurs. Therefore, the decomposition of the IFR catalyzes the TPU/IFR degradation leading to generating an intumescent and compact protective char layer. In other words, a reaction occurred in the condensed phase leading

to stabilizing the residue at high temperatures, and the TPU degradation became lower. Consequently, flame retardancy increases. Thus, the fire safety of TPU/IFR composites enhances. This approach is remarkable, and the challenges in the flame retardancy mechanism can be addressed more in future works by studying the FTIR char residues and investigating formed burning products.

FTIR analysis

Figure 13 shows the FTIR spectra of the TPU-0 and two TPU/IFR composite samples (with and without nano-silica) that exhibited the best fire performance (TPU-5, and TPU-6). The absorption peak at 3345 cm^{-1} is ascribed to $-\text{OH}$ and $-\text{N}-\text{H}$ stretching. It is reported that the proportion of $-\text{NH}$ hydrogen bonding in PUR is more than 85% of $-\text{NH}$ bonds [48]. On the other hand, this peak appeared by more intensity for TPU-6 in which there is an H-bonding between $-\text{Si}-\text{O}\dots\text{H}-$ bonds.

The absorption band at 1530 cm^{-1} can be attributed to the $-\text{N}-\text{H}$ bending and $\text{C}-\text{N}$ -stretching vibrations. The free carbonyl group at 1728 cm^{-1} and the carbonyl group bonded to the hard segments by hydrogen bonding at 1700 cm^{-1} are in good agreement with those reported in the literature [21]. As can be seen in Fig. 13, the intensity of the carbonyl peaks decreased in TPU-5 and TPU-6 samples compared to TPU-0. The absorption bands at 1309 cm^{-1} and 1220 cm^{-1} are due to $\text{C}-\text{O}$ stretching in urethane and $\text{C}-\text{O}-\text{C}$ ester stretching, respectively.

The peaks at 2919 cm^{-1} and 2931 cm^{-1} can be related to the asymmetric and symmetric stretching vibrations of $-\text{CH}$ bonds. The peaks at 1595 cm^{-1} and 770 and 820 cm^{-1} are

attributed to the aromatic structure. It means that TPU-0 was an aromatic isocyanate [49]. The absorption peaks at 1459 cm^{-1} and 1361 cm^{-1} are ascribed to the aromatic group, too [21].

In the spectrum of TPU-6, two sharp bands between 1076 cm^{-1} , 1016 cm^{-1} , and 945 cm^{-1} can be attributed to absorption bands for $\text{Si}-\text{O}-\text{Si}$ stretching in nano-silica and $\text{C}-\text{O}-\text{C}$ stretching in TPU. This observed spectrum is consistent with the IFR analysis studied on the TPU films containing nano-silica by Vega-Baudrit et al. [23].

Mechanical properties

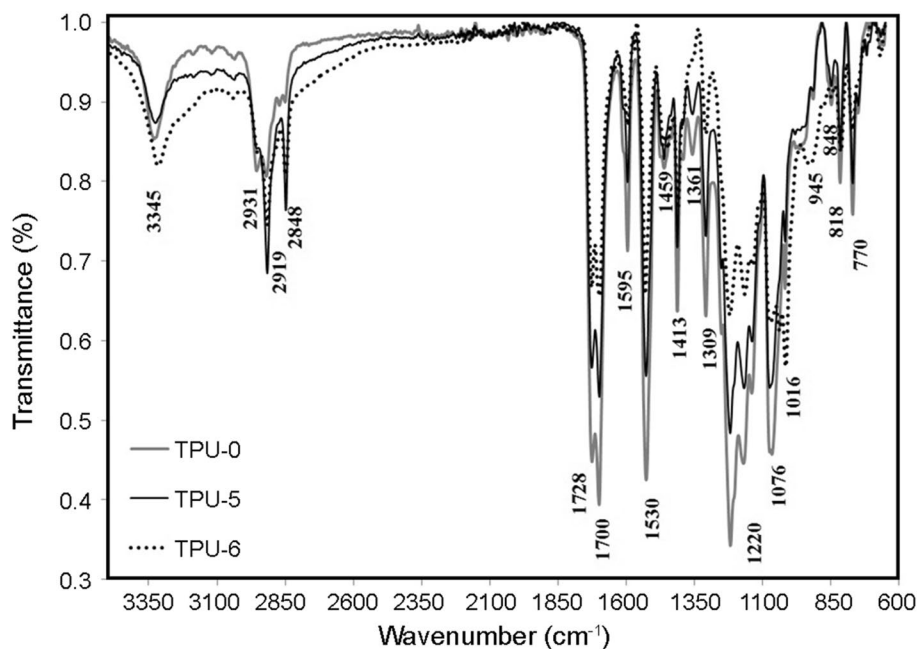
To investigate the mechanical properties of the TPU-0 and TPU/IFR composites (i.e., TPU-5 and TPU-6), three parameters were measured: 1-tensile stress (which is the magnitude F (the applied force) divided by the cross-sectional area A), 2- elongation-at-break value, and 3-shore-A hardness. These data are listed in Table 4.

Based on the results, the tensile stress of the TPU/IFR composites increased in both TPU-5 and TPU-6 samples. Tensile stress enhanced from 39 to 40 MPa in the TPU-5

Table 4 Mechanical properties of TPU and TPU/IFR composites

| Sample code | Tensile stress (MPa) | Elongation-at-break (%) | Shore A |
|-------------|----------------------|-------------------------|--------------|
| TPU-0 | 39 ± 1 | 580 ± 3 | 85 ± 1.5 |
| TPU-5 | 40 ± 1 | 560 ± 5 | 90 ± 1 |
| TPU-6 | 43 ± 1 | 550 ± 5 | 89.9 ± 1 |

Fig. 13 FTIR spectra of TPU-0, TPU-5, and TPU-6 samples



and 43 MPa in the TPU-6, respectively. It can be indicative of the good interfacial interaction between the IFR and TPU.

With the addition of 1.0 wt% of nano-silica to TPU/IFR, the tensile strength increased more. It can be attributed to the better interaction between the TPU and N-Si as well as the uniform dispersion of nano-silica. Although a downward trend of the elongation-at-break value was observed from 580% (without IFR and N-Si) to 550%–560% in flame-retardant TPU samples. For TPU-6, this reduction can be an effect of reinforcement of the matrix by nanoparticles and higher stiffness of the product. For TPU-5, this reduction is due to the restriction of the polymer chain mobility as reported by Savas et al. [50]. This phenomenon was also observed in mineral-based flame-retardant filled polymers. It was found that the tensile strength shows different trends and improvement of this parameter by clay is often reported in an elastomeric matrix [51].

Another mechanical parameter is shore hardness which is a specific parameter for elastomers and their composites. Shore-A hardness test results of the TPU-0 and TPU/IFR composites are given in Table 4. The shore hardness of both IFR-TPU samples containing IFR and nano-silica showed an enhancement. In conclusion, the data showed that the high concentration of APP in the IFR system in TPU/IFR composites did not cause deterioration of mechanical properties.

Conclusion

A highly efficient multi-component intumescent flame-retardant (IFR) system consisting of APP/MPP/PER was developed to improve the fire performance of a polyester-based TPU. TPU/IFR composites were prepared with different percentages of IFR components by the melt-mixing method. The TPU/IFR composites achieved the UL 94 V-0 grade and LOI increased up to 34.0% in the best formulation of TPU/IFR by 40 wt% APP, 10 wt% MPP, and 1 wt% PER. Significant reduction were obtained in the PHRR and peak SPR values by 80% and 90%, respectively. The incorporation of 1 wt% nano-silica into the TPU/IFR formulation with the weight ratio of APP/PER: 4/1 leads to a good flame-retardant and smoke suppression synergism in TPU/IFR composite. The LOI value reached 36%, melt dripping was removed, and the char structure was strengthened. CCT showed that the IFR system significantly reduced the PHRR and peak SPR values of the TPU nanocomposites compared to TPU/IFR by 38% and 64.5%, respectively, and enhanced fire safety with the highest FPI value, ultimately. SEM revealed the formation of a compact intumescent silica-rich char layer. The TGA results showed that both IFR-TPU samples could remarkably enhance the thermal stability of TPU/IFR composites by the char residues of 25% at 800 °C in the air. The condensed-phase flame-retardant mechanism was

confirmed based on the obtained results and the findings of previous studies in which the APP/PER complex catalyzed the degradation of IFR-TPU sample in the first stage and then promoted char formation. Mechanical test results indicated that in spite of the high loading of the IFR system, the mechanical properties of the flame-retardant TPU samples were maintained and no significant impairment was observed. Based on the results, the efficiently developed flame retardant for TPU can meet the three critical aspects of fire safety, including heat reduction, smoke suppression, and anti-dripping with reasonable fire performance without harming mechanical properties.

Acknowledgements The authors would like to thank Building and Housing Research Center (BHRC)/Fire Laboratory and Iran Polymer and Petrochemical Institute (IPPI) for supporting this research project.

Data availability Not Applicable.

References

1. Prisacariu C (2011) Polyurethane elastomers, from morphology to mechanical aspects, 1st edn. Springer-Verlag
2. Drobny JG (2014) Handbook of thermoplastic elastomers, 2nd edn. Elsevier Science
3. Tabuani D, Bellucci F, Terenzi A, Camino G (2012) Flame retarded thermoplastic polyurethane (TPU) for cable jacketing application. *Polym Degrad Stabil* 97:2594–2601. <https://doi.org/10.1016/j.polymdegradstab.2012.07.011>
4. Zhao X-L, Chen C-K, Chen X-L (2016) Effects of carbon fibers on the flammability and smoke emission characteristics of halogen-free thermoplastic polyurethane/ammonium polyphosphate. *J Mater Sci* 51:3762–3771. <https://doi.org/10.1007/s10853-015-9694-5>
5. Sut A, Metzsch-Zilligen E, Großhauser M, Pfaendner R, Scharstel B (2019) Synergy between melamine cyanurate, melamine polyphosphate and aluminum diethylphosphinate in flame retarded thermoplastic polyurethane. *Polym Test* 74:196–204. <https://doi.org/10.1016/j.polymertesting>
6. Chen X, Ma C, Jiao C (2016) Synergistic effects between iron-graphene and ammonium polyphosphate in flame-retardant thermoplastic polyurethane. *J Therm Anal Calorim* 126:633–642. <https://doi.org/10.1007/s10973-016-5494-7>
7. Lu S, Shi H, Shen B, Hong W, Yu D, Chen X (2022) Polypyrrole-functionalized g-C₃N₄ for rheological, combustion and self-healing properties of thermoplastic polyurethane. *J Polym Res* 29:263. <https://doi.org/10.1007/s10965-022-03046-x>
8. Visakh PM, Yoshihiko A (2015) Flame retardants, polymer blends, composites and nanocomposites. Springer, Cham
9. Yu G, Song M, Jiao S, Jia X, Li Y (2019) Flame retardancy of thermoplastic polyurethane using phosphorus-containing flame retardants. *IOP Conf Ser Mater Sci Eng* 585:1012038
10. Li H, Ning N, Zhang L, Wang Y, Liang W, Tian M (2014) Different flame retardancy effects and mechanisms of aluminum phosphinate in PPO, TPU and pp. *Polym Degrad Stab* 105:86–95. <https://doi.org/10.1016/j.polymdegradstab.2014.03.032>
11. Usta N (2012) Investigation of fire behavior of rigid polyurethane foams containing fly ash and intumescent flame retardant by using a cone calorimeter. *J Appl Polym Sci* 124:3372–3382. <https://doi.org/10.1002/app.35352>

12. Liu S-H, Kuan C-F, Kuan H-C, Shen M-Y, Yang J-M, Chiang C-L (2017) Preparation and flame retardance of polyurethane composites containing microencapsulated melamine polyphosphate. *Polymers* 31(9):407. <https://doi.org/10.3390/polym9090407>
13. Camino G, Costa L, Trossarelli L (1984) Study of the mechanism of intumescence in fire retardant polymers: Part I Thermal degradation of ammonium polyphosphate/pentaerythritol mixtures. *Polym Degrad Stab* 6:243–252. [https://doi.org/10.1016/0141-3910\(84\)90004-1](https://doi.org/10.1016/0141-3910(84)90004-1)
14. Wang W, Chen X, Gu Y, Jiao C (2018) Synergistic fire safety effect between nano-CuO and ammonium polyphosphate in thermoplastic polyurethane elastomer. *J Therm Anal Calorim* 131:3175–3183. <https://doi.org/10.1007/s10973-017-6724-3>
15. Wang Z, Jiang S, Sun H (2017) Expanded polystyrene foams containing ammonium polyphosphate and nano-zirconia with improved flame retardancy and mechanical properties. *Iran Polym J* 26:71–79. <https://doi.org/10.1007/s13726-016-0499-4>
16. Liu L, Xu Y, Li S, Xu M, He Y, Shi Z, Li B (2019) A novel strategy for simultaneously improving the fire safety, water resistance and compatibility of thermoplastic polyurethane composites through the construction of biomimetic hydrophobic structure of intumescent flame retardant synergistic system. *Compos Part B Eng* 176:107218. <https://doi.org/10.1016/j.compositesb.2019.107218>
17. Sinha Ray S, Okamoto M (2003) Polymer/layered silicate nanocomposites: a review from preparation to processing. *Prog Polym Sci* 28:1539–1641. <https://doi.org/10.1016/j.progpolymsci.2003.08.002>
18. Chen X, Jiang Y, Jiao C (2014) Smoke suppression properties of ferrite yellow on flame retardant thermoplastic polyurethane based on ammonium polyphosphate. *J Hazard Mater* 266:114–121. <https://doi.org/10.1016/j.jhazmat.2013.12.025>
19. Chen X, Jiang Y, Jiao C (2014) Synergistic effects between hollow glass microsphere and ammonium polyphosphate on flame-retardant thermoplastic polyurethane. *J Therm Anal Calorim* 117:857–866. <https://doi.org/10.1007/s10973-014-3831-2>
20. Martin DJ, Osman AF, Andriani Y, Edwards GA (2012). In: Gao F (ed) *Advances in polymer nanocomposites*. Woodhead Publishing
21. Saha C, Bahera PK, Raut SK, Singha NK (2021) A thermoplastic polyurethane /nanosilica composite via melt mixing process and its properties. *SILICON* 13:1041–1049. <https://doi.org/10.1007/s12633-020-00487-1>
22. Petrovic ZS, Javni I, Waddon A, Bánhegyi G (2000) Structure and properties of polyurethane-silica nanocomposites. *J Appl Polym Sci* 76:133–151. [https://doi.org/10.1002/\(SICI\)1097-4628\(20000411\)76:2%3C133::AID-APP3%3E3.0.CO;2-K](https://doi.org/10.1002/(SICI)1097-4628(20000411)76:2%3C133::AID-APP3%3E3.0.CO;2-K)
23. Vega-Baudrit J, Sibaja-Ballesteros M, Martín-Martínez JM (2009) Study of the relationship between nanoparticles of silica and thermoplastic polymer (TPU) in nanocomposites. *Nanotech Prog Int* 1:24–34
24. Yuan Y, Yang H, Yu B, Shi Y, Wang W, Song L, Hu Y, Zhang Y (2016) Phosphorus and nitrogen-containing polyols: synergistic effect on the thermal property and flame retardancy of rigid polyurethane foam composites. *Ind Eng Chem Res* 55:10813–10822. <https://doi.org/10.1021/acs.iecr.6b02942>
25. Yang W, Yuen RKK, Hu Y, Lu H, Song L (2011) Development and characterization of fire retarded glass-fiber reinforced poly (1, 4-butylene terephthalate) composites based on a novel flame retardant system. *Ind Eng Chem Res* 50:11975–11981. <https://doi.org/10.1021/ie201550z>
26. Zhao KM, Xu WZ, Song L, Wang BB, Feng H, Hu Y (2012) Synergistic effects between boron phosphate and microencapsulated ammonium polyphosphate in flame-retardant thermoplastic polyurethane composites. *Polym Adv Technol* 23:894–900. <https://doi.org/10.1002/pat.1985>
27. Bakhtiyari S, Taghi-Akbari L, Jamali Ashtiani M (2015) Evaluation of thermal fire hazard of 10 polymeric building materials and proposing a classification method based on cone calorimeter results. *Fire Mater* 39:1–13. <https://doi.org/10.1002/fam.2219>
28. Gou JH, Tang Y (2010) Flame retardant polymer nanocomposites. In: Leng J, Lau AKT (eds) *Multifunctional polymer nanocomposites*, 1st edn. CRC Press, Boca Raton. <https://doi.org/10.1201/b10462>
29. Babrauskas V, Peacock R (1990) Heat release rate: the single most important variable in fire hazard. *Fire Retardant Chemicals Association (FRCA)*
30. Duquesne S, Le Bras M, Bourbigot S, Delobel R, Camino G, Eling B, Lindsay C, Roels T, Vezin H (2001) Mechanism of fire retardancy of polyurethanes using ammonium polyphosphate. *J Appl Polym Sci* 82:3262–3274. <https://doi.org/10.1002/app.2185>
31. Wang Z, Jiang Y, Yang X, Zhao J, Fu W, Wang N, Wang D-Y (2022) Surface modification of ammonium polyphosphate for enhancing flame-retardant properties of thermoplastic polyurethane. *Materials* 15:1990. <https://doi.org/10.3390/ma15061990>
32. Li H, Huo C, Miao P, Zhang T, Wei H (2017) Phenolic foam based the influence of intumescent flame retardancy system ammonium polyphosphate/pentaerythritol/melamine. In: *Advances in Engineering*, Vol.100. Proceedings of International Conference on Manufacturing Engineering and Intelligent Materials (ICMEIM 2017)
33. Weil ED (1992) Synergists, adjuvants and antagonists in flame-retardant systems. In: Lewin M (ed) *Proceedings of conference on recent advance flame retard polymer mater*. BCC Inc, Norwalk
34. Xia Y, Jin F, Mao Z, Guan Y, Zheng A (2014) Effects of ammonium polyphosphate to pentaerythritol ratio on composition and properties of carbonaceous foam deriving from intumescent flame-retardant polypropylene. *Polym Degrad Stab* 107:64–73. <https://doi.org/10.1016/j.polymdegradstab.2014.04.016>
35. Bourbigot S, Turf T, Bellayer S, Duquesne S (2009) Polyhedral oligomeric silsesquioxane as flame retardant for thermoplastic polyurethane. *Polym Degrad Stab* 94:1230–1237. <https://doi.org/10.1016/j.polymdegradstab.2009.04.016>
36. Almeras X, Bras ML, Hornsby P, Bourbigot S, Marosi G, Keszei S, Poutch F (2003) Effect of fillers on the fire retardancy of intumescent polypropylene compounds. *Polym Degrad Stab* 82:325–331. [https://doi.org/10.1016/S0141-3910\(03\)00187-3](https://doi.org/10.1016/S0141-3910(03)00187-3)
37. Jiao CM, Chen XL (2010) Flammability and thermal degradation of intumescent flame-retardant polypropylene composites. *Polym Eng Sci* 50:767–772. <https://doi.org/10.1002/pen.21583>
38. Ditrlich B, Wartig KA, Mühlaupt R, Scharfel B (2014) Flame-retardancy properties of intumescent ammonium poly (phosphate) and mineral filler magnesium hydroxide in combination with graphene. *Polymers* 6:2875–2895. <https://doi.org/10.3390/polym6112875>
39. Yang A-H, Deng C, Chen H, Wei Y-X, Wang Y-Z (2017) A novel Schiff-base polyphosphate ester: highly-efficient flame retardant for polyurethane elastomer. *Polym Degrad Stab* 144:70–82. <https://doi.org/10.1016/j.polymdegradstab.08.007>
40. Chen X, Jiang Y, Liu J, Jiao C, Qian Y, Li S (2015) Smoke suppression properties of fumed silica on flame-retardant thermoplastic polyurethane based on ammonium polyphosphate. *J Therm Anal Calorim* 120:1493–1501. <https://doi.org/10.1007/s10973-015-4424-4>
41. Sonnier R, Vahabi H, Chivas-Joly C (2019) New insights into the investigation of smoke production using a cone calorimeter. *Fire Technol* 55:853–873. <https://doi.org/10.1007/s10694-018-0806-z>
42. Ricciardi MR, Antonucci V, Zarrelli M, Giordano M (2012) Fire behavior and smoke emission of phosphate-based inorganic fire-retarded polyester resin. *Fire Mater* 36:203–215. <https://doi.org/10.1002/fam.1101>

43. Liu L, Zhao X, Ma C, Chen X, Li S, Jiao C (2016) Smoke suppression properties of carbon black on flame retardant thermoplastic polyurethane based on ammonium polyphosphate. *J Therm Anal Calorim* 126:1821–1830. <https://doi.org/10.1007/s10973-016-5815-x>
44. Herrera M, Matuschek G, Kettrup A (2002) Thermal degradation of thermoplastic polyurethane elastomers (TPU) based on MDI. *Polym Degrad Stab* 78:323–331. [https://doi.org/10.1016/FS0141-3910\(02\)00181-7](https://doi.org/10.1016/FS0141-3910(02)00181-7)
45. Morgan AB (2019) The future of flame retardant polymers – unmet needs and likely new approaches. *Polym Rev* 59:25–54. <https://doi.org/10.1080/15583724.2018.1454948>
46. Lim K-S, Bee S-T, Sin L-T, Tee T-T, Ratnam C-T, Hui D, Rahmat AR (2016) A review of application of ammonium polyphosphate as intumescent flame retardant in thermoplastic composites. *Compos Part B Eng* 84:155–174. <https://doi.org/10.1016/j.compositesb.2015.08.066>
47. Levchik SV, Weil ED (2004) Thermal decomposition, combustion and fire-retardancy of polyurethanes—a review of the recent literature. *Polym Int* 53:1585–1610. <https://doi.org/10.1002/pi.1314>
48. Cui Y, Pan H, Zhang J, Cao L, Zong C (2022) Influence of polydimethylsiloxane on the microstructure and properties of polyester thermoplastic polyurethane. *J Polym Res* 29:218. <https://doi.org/10.1007/s10965-022-03079-2>
49. Cai C, Sun Q, Zhang K, Bai X, Liu P, Li A, Yu ZL, Li Q (2022) Flame-retardant thermoplastic polyurethane based on reactive phosphonate polyol. *Fire Mater* 46:130–137. <https://doi.org/10.1002/fam.2959>
50. Savas LA, Deniz TK, Tayfun U, Dogan M (2017) Effect of microcapsulated red phosphorus on flame retardant, thermal and mechanical properties of thermoplastic polyurethane composites filled with huntite&hydromagnesite mineral. *Polym Degrad Stab* 135:121–129. <https://doi.org/10.1016/j.polyimdeggradstab.2016.12.001>
51. Zaman I, Manshoor B, Khalid A, Araby S (2014) From clay to graphene for polymer nanocomposites—a survey. *J Polym Res* 21:429. <https://doi.org/10.1007/s10965-014-0429-0>

Springer Nature or its licensor (e.g. a society or other partner) holds exclusive rights to this article under a publishing agreement with the author(s) or other rightsholder(s); author self-archiving of the accepted manuscript version of this article is solely governed by the terms of such publishing agreement and applicable law.

Authors and Affiliations

Leila Taghi-Akbari¹ · Mohammad Reza Naimi-Jamal¹  · Shervin Ahmadi²

✉ Mohammad Reza Naimi-Jamal
naimi@iust.ac.ir

Leila Taghi-Akbari
taghiakbari_l@chem.iust.ac.ir

¹ Department of Chemistry, Iran University of Science and Technology (IUST), Tehran 16846-13114, Iran

² Iran Polymer and Petrochemical Institute (IPPI), Tehran 14965-115, Iran